Towards a model-independent determination of the $\phi \to \gamma f_0$ coupling

M. Boglione, M.R. Pennington

Institute for Particle Physics Phenomenology, University of Durham, Durham, DH1 3LE, UK

Abstract. A guide to the composition of the enigmatic $f_0(980)$ and $a_0(980)$ states is their formation in ϕ-radiative decays. Precision data are becoming available from the KLOE experiment at the DAΦNE machine at Frascati, as well as results from SND and CMD-2 at VEPP-2M at Novosibirsk. We show how the coupling of the $f_0(980)$ to this channel can be extracted from these, independently of the background provided by σ production. To do this we use the fact that the behaviour of both the $f_0(980)$ and σ cannot be determined by these data alone, but is strongly constrained by experimental results from other hadronic processes as required by unitarity. We find that the resulting coupling for the $\phi \to \gamma f_0(980)$ is $\sim 10^{-4}$ GeV with a background that is quite unlike that assumed if unitarity is neglected. This provides an object lesson in how unitarity teaches us to add resonances. Not surprisingly the result is crucially dependent on the pole position of the $f_0(980)$, for which there are still sizeable uncertainties. At present this leads to an uncertainty in the $\phi \to \gamma f_0$ branching ratio which can only be fixed by further precision data on the $f_0(980)$. Nevertheless, the BR($\phi \to \gamma f_0$) is now the same order of magnitude as the experimental BR($\phi \to \gamma a_0$).

1 Introduction

Much has been written about the possible nature of the $f_0(980)$ and $a_0(980)$ states. Are they conventional $q\bar{q}$ scalars, or $K\overline{K}$ molecules, or four-quark states? Are these two states with almost degenerate masses closely related, or is the degeneracy just an accident?

A clue to the composition of these states is provided by the way they appear in ϕ-radiative decays. The ϕ provides us with a clean $s\bar{s}$ system, which picks out the components of each of these states that couples to strangeness, even though their masses are below $K\overline{K}$ threshold. Consequently, the $f_0(980)$, in particular, appears as a peak in the $\pi\pi$ decay distribution, as seen in $\psi \to \phi(\pi\pi)$ or $D_s \to \pi(\pi\pi)$, while in channels in which the $f_0(980)$ is produced from predominantly non-strange quarks, as in $\pi\pi \to \pi\pi$ scattering or in central di-pion production with pion or proton beams, it appears as a dip or a shoulder.

The absolute values of the branching ratio for $\phi \to \gamma f_0/a_0$, as well as the ratio of these, has been advertised in the past as a guide to distinguish $n\bar{n}$ from $s\bar{s}$ from $K\overline{K}$ and $qq\bar{q}\bar{q}$ systems, as summarised in Table 1 [1,2].

According to this, the first results from the two VEPP-2M experiments at Novosibirsk [3–5] indicate a four-quark composition. However, it is now known that the strong suppression of the $\phi \to \gamma f_0$ branching ratio in the molecular models indicated in Table 1 is wholly because of oversimplified modelling of the decay process in this case, as

Table 1. Predictions for the absolute rate for $\phi \to \gamma f_0(980)$ depending on the composition of the $f_0(980)$ [1,2]

Composition	BR($\phi \to \gamma f_0(980)$)
$qq\bar{q}\bar{q}$	$O(10^{-4})$
$s\bar{s}$	$O(10^{-5})$
$K\overline{K}$	$< O(10^{-5})$

pointed out by Oller [6], so any conclusion about a four-quark composition is far from certain.

The $\eta\pi$-channel by which the a_0 is identified is clean with very little background, either background from competing 7γ final states, but also from other hadronic states — none are nearby. In contrast the $f_0(980) \to \pi^0\pi^0$ decay gives a final state that has an experimental background from $\rho^0\pi^0$, where the $\rho^0 \to \gamma\pi^0$, as well as a significant contribution from the production of $\sigma \to \pi^0\pi^0$. These backgrounds mean that the extraction of the $\phi \to \gamma f_0(980)$ signal depends on our ability to separate the different components. The $\rho\pi$ signal is characterised by a different angular dependence than that for γf_0. The former is flat in $\cos\theta$, while the latter has a $(1 + \cos^2\theta)$ distribution. The KLOE data [7] reveal that the $\rho\pi$ component is essentially negligible and we will take that as read. To separate the different scalar $\pi\pi$ components, in particular the σ from the $f_0(980)$, models of these two states are used. Since the ϕ-radiative decay data alone cannot deter-

mine the masses and widths of these resonances, their key parameters are taken to be fixed by other experiments.

For instance, the KLOE collaboration have made a determination of the BR($\phi \to \gamma f_0$) from their own data and found this to be $4.5 \cdot 10^{-4}$, while the corresponding value for BR($\phi \to \gamma a_0$) is a factor (6.1 ± 0.6) smaller [8]. So why is the reanalysis presented here necessary? Firstly, the KLOE group adjust the $f_0(980)$ mass and width to give the best fit to their data. This results in a mass of $969\,\mathrm{MeV}$ with a width of 150–$250\,\mathrm{MeV}$. This width is, as we shall recall shortly, far larger than other determinations of the $f_0(980)$ width, which are typically $50\,\mathrm{MeV}$ (see for example [9]). Consequently, their f_0 peak sweeps in a larger range of $\pi\pi$ production and this inevitably leads to a very large value for the BR($\phi \to \gamma f_0$). Clearly a more conventional f_0 width would mean that the significant production of two pions with mass of 800–$900\,\mathrm{MeV}$ must come from some other source than the $f_0(980)$. Having adjusted the parameters to maximize the agreement with their data, the KLOE group then add a σ contribution, where the parameters for this low mass $\pi\pi$ enhancement is taken from the maximum likelihood fit by Fermilab-E791 to their $D \to 3\pi$ data. The E791 analysis is cast into doubt by the implied phase of their S-wave $\pi\pi$ production amplitudes not being consistent with the phase determined in the $\pi\pi$ elastic scattering. Moreover, KLOE just add this contribution to that of their broad $f_0(980)$ with no regard for the quantum mechanical bound that probabilities must not exceed 100%, i.e. they violate *unitarity*. The KLOE data alone cannot determine the parameters of both the σ and of the $f_0(980)$. Consequently, we embark on a new determination of BR($\phi \to \gamma f_0$) which automatically embodies coupled-channel unitarity and is in accord with meson scattering information on $\pi\pi$ and $K\overline{K}$ production. We than use the ϕ-radiative decay datasets to fix the relevant couplings.

If the resonant states that contributed to the decay $\phi \to \gamma\pi\pi$ were narrow and well-separated then the branching ratio to any of these could be established by simply fitting data with appropriate Breit–Wigner forms. However, the scalar $f_0(980)$ overlaps with the notoriously broad $f_0(400$–$1200)$ (or σ), and couples strongly to the $K\overline{K}$ channel that opens within its width. Moreover, since below $1\,\mathrm{GeV}$ the $\pi\pi$ channel is effectively the only open hadronic channel, unitarity is a particularly powerful constraint. This requires all processes in which a di-pion system is produced to have closely related final state interactions – a relationship embodied in Watson's famous theorem. Consequently, the S-wave $\pi\pi$ system produced in ϕ-radiative decay is already exposed in other hadronic processes, particularly high energy reactions where the di-pions are either peripherally or centrally produced. Only if the states in this system were narrow and well-separated would fitting be a matter of taking Breit–Wigners with couplings to be determined as the KLOE group do.

The coupling of a resonance is only determined independently of any other resonance with which it may overlap, or independently of any non-resonant background, by continuing the resulting $\phi \to \gamma\pi\pi$ amplitude into the com-

plex s plane to the f_0 pole on the appropriate unphysical sheet. The residue of the pole gives the coupling and this is the only model-independent parameter that can be determined. In the case of a narrow isolated resonance this coupling given by the pole residue is directly related to a branching ratio. Where states are not narrow, or overlap with each other or with strongly coupled thresholds, the branching ratio is only related to this coupling in a model-dependent way, unless one has data of infinite precision. Consequently the $\phi \to \gamma\pi\pi$ branching ratios we quote are (like those of all authors) subject to model dependence of the f_0 line shape.

2 Unitarity and underlying hadronic amplitudes

Unitarity has to be respected. The natural way to ensure this is to represent the purely hadronic scattering amplitudes with definite angular momentum by the T-matrix and express this in terms of a real K-matrix. Then with ρ the diagonal phase space matrix, we have

$$T \;=\; K\,(I - \mathrm{i}\,\rho\,K)^{-1} \quad . \tag{1}$$

The amplitude F describing the production of the same final state with the same quantum numbers is then related to the T-matrix, provided the "production" process has no other strongly interacting final states, or as in an isobar picture one assumes only isobar interactions with negligible three- or more body interactions. The relation between F and T is then implemented using either the P-vector or Q-vector (here called equivalently the $\alpha-$coupling vector), so that

$$F \;=\; P\,(I - \mathrm{i}\,\rho\,K)^{-1} \;=\; \alpha\,T \quad . \tag{2}$$

There are constraints on P and α, which have to be satisfied. Firstly,

(1) P and α are real vectors;
(2) if the K-matrix elements have poles, then these must also appear in the P-vector;
(3) while the latter constraint is automatically built into the coupling vector representation, care must instead be taken of the zeros of the T-matrix elements. Thus α has poles to remove any real zeros of the T-matrix, or its determinant.

The P-vector and α-vector formulations are, of course, equivalent. They each embody the *universality* that demands that poles of the S-matrix transmit to all processes with the same quantum numbers in exactly the same position. That this is a fundamental S-matrix principle has been questioned in a series of papers by the Ishidas [10], as being incompatible with quark dynamics. However the principle of universality is a consequence of causality and the conservation of probability for hadronic reactions totally independently of the underlying dynamics of the supposed constituents of hadrons. This universality is not an optional constraint or a matter of debate. It is a rigorous consequence of fundamental principles that define what is meant by the hadron spectrum. This universality of strong

interactions applies to ϕ-radiative decay, since the photon–hadron interaction is electromagnetic, and the ϕ and π are presumed to have negligible strong interactions.

Though the P-vector and α-vector formulations are equivalent and translatable one-to-one, one form may be easier to implement in practice than the other. We will use the coupling vector formulation. In the energy range accessed in ϕ-radiative decay, the only hadronic intermediate states that can possibly enter into $\pi\pi$ production are $\pi\pi$ and $K\overline{K}$. Consequently we introduce two functions α_1 and α_2, which represent the coupling of the ϕ to $\gamma\pi\pi$ and $\gamma K\overline{K}$, respectively. Provided these functions are real for $\pi\pi$ energies above threshold, then two-channel unitarity is satisfied by construction.

The amplitude, F, for S-wave di-pion production in ϕ-radiative decay is thus related to the two hadronic scattering amplitudes, T_{11} for $\pi\pi \to \pi\pi$, and T_{12}, for $\pi\pi \to K\overline{K}$. " 1" labels the $\pi\pi$ channel and "2" the $K\overline{K}$, and time reversal invariance implies that $T_{12} = T_{21}$. Each amplitude and coupling function depends on s, the square of the mass of the di-pion system. Then unitarity requires

$$F(s) = \alpha_1(s)\, T_{11}(s) + \alpha_2(s)\, T_{12}(s) \quad . \qquad (3)$$

The hadronic elements T_{ij} typically have real Adler zeros at $s = s_{ij}$, and the two channel determinant $T_{11} T_{22} - T_{12}^2$ may have a real zero at $s = s_T$. These zeros do not in general transmit to the decay or production amplitude, being process specific. The Adler zeros of the hadronic amplitudes are, in the analyses we use, taken to be at the same position so $s_{11} = s_{12} = s_{22} = s_0$. Moreover, the decay amplitude for $\phi \to \gamma(\pi\pi)$ is expected to have its own (process-dependent) Adler zero at $s = s_A$. Consequently, the coupling functions are parametrised to incorporate this zero, while eliminating those in the underlying T-matrix elements and their two channel determinant, in the following straightforward way:

$$\alpha_1(s) = \frac{(s - s_A)}{(s - s_0)} \left\{ p_1(s) + \frac{\beta}{(s - s_T)} \right\} \ ,$$
$$\alpha_2(s) = \frac{(s - s_A)}{(s - s_0)} \left\{ p_2(s) - \frac{\beta\, r_T}{(s - s_T)} \right\} \ , \qquad (4)$$

where β is a dimensionful constant, $r_T = T_{11}(s_T)/T_{12}(s_T)$ and the $p_i(s)$ are expected to be represented by low order polynomials – all real.

For the hadronic T-matrix we will use a K-matrix analysis of meson production by Morgan and Pennington which updates the AMP analysis of [11] with the constraints on near $K\overline{K}$ threshold production of [12]. This is referred to as the ReVAMP analysis. The hadronic amplitudes embody the information we have on the structure of the $f_0(600)$ (or σ) and the $f_0(980)$. Even though this is an old analysis, the features of the embedded $f_0(980)$ (pole position, mass and width) are in excellent agreement with the most recent data on D_s decays into pions. The interpretation of these in terms of possible quark structure is then to be elucidated by the coupling of the $\phi \to \gamma f_0$.

Later we will compare the fits obtained using this set of underlying amplitudes with those found by using a second

Table 2. Pole position on sheet II with the $\pi\pi$, $K\overline{K}$ couplings and widths relative to the $f_0(980)$ embedded in the two different schemes ReVAMP [12] and AS [13]. Note that in the AS underlying amplitudes the $f_0(980)$ is a much broader resonance than in the ReVAMP amplitudes

	ReVAMP	AS
Pole (MeV)	$E_R = (988 - \mathrm{i} \cdot 23)$	$E_R = (1024 - \mathrm{i} \cdot 43)$
g_π (MeV)	163	328
g_K (MeV)	173	398
Γ_π (MeV)	25	98
Γ_K (MeV)	3	36

input, from a much more complete and much more recent analysis of a wide range of di-meson production data by Anisovich and Sarantsev [13]. This we reference as the AS analysis. The two sets of hadronic amplitudes, ReVAMP and AS have quite different parameters for the $f_0(980)$, see Table 2, and this difference leads to distinct $\phi \to \gamma f_0$ couplings, as we will discuss in Sect. 5.

It is important to appreciate that hadronic data may well be fitted equally well by several K-matrix parametrisations. The resulting T-matrix elements will be identical within experimental uncertainties and should provide the same poles of the T-matrix. However, depending on how the underlying K-matrix is described in terms of poles alone, or poles plus some background, the poles of the K-matrix may be quite different in number and in quite different positions. This is of no physical consequence. However, it clearly does have consequences for those that identify the poles of the K-matrix with underlying bare states [14]. It is important to realise that this is a modelling that may or may not accord with QCD. Having a range of K-matrix parametrisations of the same data recognises that we cannot yet calculate in detail the strong physics aspects of QCD. Only if one desires to imbue the K-matrix elements themselves with significance is it necessary to ensure that the K-matrix elements have the correct left hand cut analyticity, whilst fitting along the right hand cut. If the elements are just a convenient way of parametrising data along the unitarity cut, then approximating distant left hand cut effects by poles and a polynomial background is sufficiently general.

Though the hadronic amplitudes ReVAMP and AS are the results of fits to similar datasets on $\pi\pi$ and $K\overline{K}$ production data, they have quite different parameters for the $f_0(980)$ as indicated by the pole positions; see Table 2. (The precise definition of the quantities g_π, Γ_π and g_K, Γ_K will be explained later.) To understand the differences in these two versions of the $f_0(980)$ we show the underlying $\pi\pi$ amplitude T_{11} as computed in the ReVAMP and in the AS scheme, compared with the CERN–Munich [15], BNL-E852 [16] and BNL-E856 [17] data. By comparing the solid and dashed lines it is immediately apparent that the $f_0(980)$ embedded in the AS amplitudes, which is responsible for the dip in the $I = J = 0$ $\pi\pi \to \pi\pi$ cross-section, is a much broader resonance than in the ReVAMP amplitudes. Moreover, as we can see in Table 2, in the AS

scheme the $f_0(980)$ corresponds to a pole situated above the $K\overline{K}$ threshold and has a mass larger than the mass of the ϕ, $\mathrm{Re}E_R > m_\phi$, as opposed to the ReVAMP's f_0. These differences will critically influence the calculation of the $\phi \to \gamma f_0$ coupling, obtained by continuing the amplitude $F(s)$ into the complex energy plane on the second sheet to the $f_0(980)$ pole, as will be evident in Sect. 5.

3 The fit

Based on (3) and (4), our simultaneous fits to the experimental data are performed using the expression

$$\frac{\mathrm{d}\Gamma(\phi \to \gamma f_0)}{\mathrm{d}E} = \rho(s)\,|F(s)|^2\,, \qquad (5)$$

which relates the experimental decay rate to the amplitude $F(s)$. Here $\sqrt{s} = E = M_{\pi\pi}$ is the invariant mass of the di-pion system; $\rho(s)$ is the appropriate three-body phase space for the decay $\phi \to \gamma(\pi\pi)$:

$$\rho(s) = \frac{\pi^2}{2m_\phi^3}\,(m_\phi^2 - s)\sqrt{s - 4m_\pi^2}\,, \qquad (6)$$

and $F(s)$ is the complex amplitude, which is related by unitarity to the hadronic amplitudes $T_{11}(s)$ and $T_{12}(s)$ through (3). The data, of course, know about gauge invariance of the photon field and so the fits require the coupling functions $\alpha_i(s)$ to have a zero at $s = m_\phi^2$. However, the fitting is aided by building in this consequence of gauge invariance from the start and so we introduce a factor of $(1 - s/m_\phi^2)$, where m_ϕ here is the value of the c.m. energy to which the initial e^+e^- beams are tuned (see [19] for details). Consequently we construct the decay amplitude of (3) using

$$\alpha_1(s) = \frac{(s - s_A)}{(s - s_0)}\left\{p_1(s) + \frac{\beta}{(s - s_T)}\right\}\left(1 - \frac{s}{m_\phi^2}\right)\,,$$

$$\alpha_2(s) = \frac{(s - s_A)}{(s - s_0)}\left\{p_2(s) - \frac{\beta\,r_T}{(s - s_T)}\right\}\left(1 - \frac{s}{m_\phi^2}\right)\,, \qquad (7)$$

where β together with the coefficients of the polynomials $p_1(s)$ and $p_2(s)$ are the parameters of the fit. The AS hadronic amplitudes have no zero in their two channel T-matrix determinant. Consequently, in this case $\beta = 0$, or equivalently $s_T \to \infty$.

The position of the Adler zero required by chiral dynamics is expected to be $s_A = \mathcal{O}(m_\pi^2)$. However, our fits prove insensitive to its exact position, so we simply fix $s_A = 0$.

The polynomials $p_i(s)$ are in general to be as little structured as possible consistent with the fitting of the data. Using the ReVAMP set of underlying hadronic amplitudes, a satisfactory fit is obtained by simply using $p_i(s)$ of zeroth order in s, i.e. constant:

$$p_1(s) = a_1\,,$$
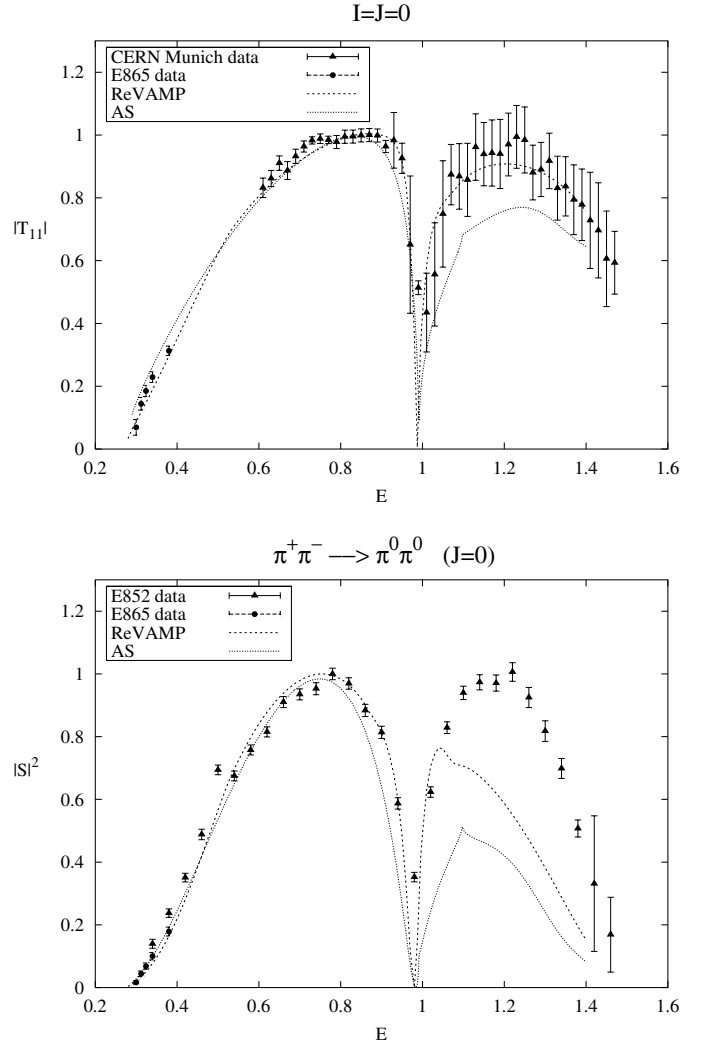$$p_2(s) = a_2\,. \qquad (8)$$

Fig. 1. The $\pi\pi$ underlying amplitudes as obtained from the ReVAMP parametrisation (solid line) and from the AS parametrisation (dashed line) are compared to two sets of experimental data. In the upper picture the modulus of the isospin zero amplitude T_{11} is plotted on top of the results of the Ochs–Wagner analysis of the CERN-Munich data [15]. In the lower picture the modulus squared of the $\pi\pi$ S-wave (which includes the contribution from the $I = 2$ channel [18]) is plotted on top of the BNL-E852 data of [16]. On both plots the low energy data (circles) correspond to the BNL-E865 measurement of K_{e4}^+ decays [17]. Differences between the data and the $\pi\pi$ amplitudes is attributed to non-pion exchange contributions to di-pion production, which are markedly different in the two cases

The line shape obtained from this fit, labeled by ReVAMP-0 (where 0 indicates the order of the polynomial in the α) is shown in Fig. 2, together with the data points from KLOE [7] and from a recent reanalysis of SND [5]. All the fits are performed by integrating the theoretical expression over each experimental mass bin. This is important where the amplitude and phase space are varying rapidly within a given experimental bin. The values of χ^2 and free parameters determined by this fit are shown in the first
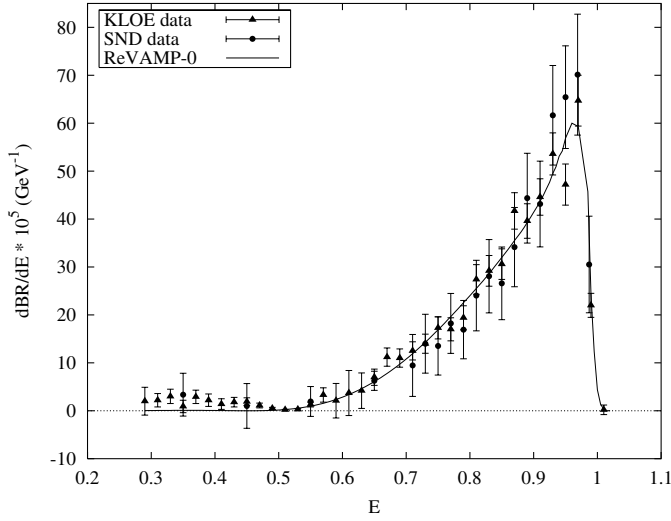
Fig. 2. Simultaneous fits to KLOE [7] and SND [5] data as obtained by using the ReVAMP [11,12] set of underlying amplitudes, with constant $p_i(s)$
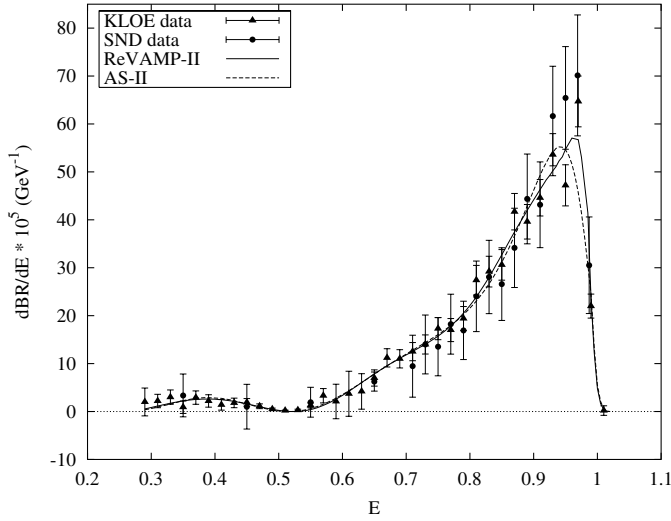

Fig. 3. Simultaneous fits to KLOE [7] and SND [5] data as obtained by using the ReVAMP [12] (solid line) and the AS [13] (dashed line) underlying amplitudes, with $p_i(s)$ polynomials of second order in s

Table 3. Values of the free parameters as determined by our fits to KLOE + SND data corresponding to the ReVAMP and AS parametrisation for the underlying amplitudes T_{11} and T_{12}, and to α polynomials of either zeroth or second order

	ReVAMP-0	ReVAMP-II	AS-II
$\chi^2/$d.o.f. - KLOE	1.60	0.82	1.28
$\chi^2/$d.o.f. - SND	0.52	0.62	0.59
$a_1 \cdot 10^2$	0.27	0.51	0.22
$b_1 \cdot 10^2$	–	−1.19	−3.08
$c_1 \cdot 10^2$	–	0.83	4.89
$a_2 \cdot 10^2$	−0.07	−3.44	−10.09
$b_2 \cdot 10^2$	–	11.94	28.43
$c_2 \cdot 10^2$	–	−10.45	−14.24
$\beta \cdot 10^2$	0.21	0.13	–

probable. However, we are aware that the AS amplitudes are the result of studying a far more comprehensive set of hadronic data than the older analysis included in ReVAMP and it is for this reason and that alone that we include the results using the AS amplitudes. Since the AS and ReVAMP differ significantly for complex values of energy away from the real axis where our fits are performed, see Fig. 5, these differences have an appreciable effect on the coupling g_ϕ of $\phi \to \gamma f_0$, as we will discuss in more detail in the Sect. 5.

In the second and third rows of Table 3 we compare the values of $\chi^2/$d.o.f. and of the free parameters as determined by our second order fits relative to each choice of underlying amplitudes, indicated as ReVAMP-II and AS-II, and in Fig. 3 the line shapes obtained from these fits are compared with the experimental data from KLOE [7] and SND [5].

Notice that global fits to all four sets of available data on ϕ-radiative decay, KLOE [7], SND [4,5] and CMD-2 [3] are dominated by the smaller error bars from KLOE and the reanalysed SND [5], so that these fits are indistinguishable from those of Figs. 2 and 3. The KLOE data at least are presumed to be free of $\phi \to \gamma\pi$ background.

column of Table 3. The quality of the fit is excellent indicating that the assumption of no significant strong $\phi\pi$ interactions is satisfactory.

In contrast, when underlying amplitudes from the AS set are used, second order $p_i(s)$ polynomials are needed to reach a quality comparable to that of the ReVAMP-0 fit:

$$p_1(s) = a_1 + b_1 s + c_1 s^2 ,$$
$$p_2(s) = a_2 + b_2 s + c_2 s^2 , \qquad (9)$$

as $\chi^2/$d.o.f. is still as big as 4 for first order p_is.

The ReVAMP amplitudes provide an excellent fit to the radiative ϕ decay data, far better than the comparable fits using the latest AS amplitudes. On chi-squared grounds alone the latter would be ruled out as quite im-

4 Determination of the couplings

The coupling g_ϕ, which governs the decay of ϕ into $f_0(980)$, is calculated by continuing the amplitude $F(s)$ into the complex s plane to the position of the f_0 pole (which is determined by the underlying amplitudes' denominator). This procedure ensures the absence of any background contamination. The pole residue is then evaluated from the strong interaction amplitudes $T(s)$, and the radiative decay amplitude $F(s)$, which are both pole dominated in the neighbourhood of the resonance pole itself, i.e. for $s \sim s_R$

$$T_{11}(s) = \frac{g_\pi^2}{s_R - s} , \qquad (10)$$

$$F(s) = \frac{g_\phi \, g_\pi}{s_R - s} . \qquad (11)$$

Table 4. Values of the branching ratio BR($\phi \to \gamma f_0(980)$) and of the g_ϕ couplings corresponding to different fits to KLOE and SND data using the ReVAMP [12] and AS [13] underlying hadronic amplitudes. Note that BR($\phi \to \gamma f_0 \to \gamma \pi^0 \pi^0$) has been multiplied by a factor three to obtain BR($\phi \to \gamma f_0(980)$) to take into account the contribution of the charged pions decay mode of the $f_0(980)$

	ReVAMP-0	ReVAMP-II	AS-II
$g_\phi \cdot 10^4$ (GeV)	6.21	6.50	18.66
BR($\phi \to \gamma f_0$) $\cdot 10^4$	0.31	0.34	1.92

Thanks to the parametrisation of the T in terms of the K-matrix, we know their numerators and denominators

$$T_{11}(s) = \frac{N_\pi(s)}{D(s)}, \quad T_{12}(s) = \frac{N_K(s)}{D(s)}, \qquad (12)$$

and consequently we have

$$F(s) = \frac{\alpha_1(s)N_\pi(s) + \alpha_2(s)N_K(s)}{D(s)}. \qquad (13)$$

In the region nearby $s = s_R$ we can write a Taylor expansion of the function $D(s)$ truncated at the first order

$$D(s \sim s_R) \sim D(s_R) + D'(s_R)(s - s_R) = D'(s_R)(s - s_R), \qquad (14)$$

since $D(s_R) = 0$ at the resonance pole. By substituting this into (12) and comparing with (10) and (11), we find

$$g_\pi = \sqrt{\frac{N_\pi(s_R)}{D'(s_R)}}, \qquad (15)$$

$$g_\phi = \frac{1}{g_\pi} \frac{\alpha_1(s_R)N_\pi(s_R) + \alpha_2(s_R)N_K(s_R)}{D'(s_R)}. \qquad (16)$$

Knowing the $\phi \to \gamma f_0$ coupling g_ϕ is the key result of our analysis shown in Table 4. It is this that is model-independent and so can be compared with predictions from different modellings of the make-up of the $f_0(980)$.

4.1 Suppression effect of the photon momentum

There is one delicate but crucial point we want to underline. What we are studying here is the radiative decay of the ϕ. This means that the corresponding amplitude $F(s)$ includes a factor given by the momentum of the radiated photon $k \propto (1 - s/m_\phi^2)$, which we have included in the α coefficients; see (7). Now, it is easy to see how this factor produces a very strong suppression in $F(s)$ in the energy region around 1 GeV, exactly where one calculates the value of the $\phi \to \gamma f_0$ coupling g_ϕ. To make it clear we construct the amplitude $\overline{F}(s)$ which one would obtain if the photon momentum factor was divided out of the α. The plots in Fig. 4 illustrate this suppression. Let us see the details. $F(s)$ is constructed from $T_{11}(\pi\pi \to \pi\pi)$ and $T_{21}(K\overline{K} \to \pi\pi)$ with weights given by the coupling functions α_1 and α_2 respectively, according to (3). In the region

around 1 GeV, the amplitude $|T_{11}|$, Fig. 4a, has a sharp dip, whereas $|T_{12}|$, Fig. 4b, shows a pronounced peak (both structures signal the presence of the $f_0(980)$). Because of the peak in the 1 GeV energy region of the $\phi \to \gamma f_0$ spectrum, one expects the couplings α_1, α_2 make the contribution of $|T_{21}(K\overline{K} \to \pi\pi)|$ dominate over $|T_{11}(\pi\pi \to \pi\pi)|$ in that region. Though $\overline{F}(s)$ seen in Fig. 4c shows the dominance of $\alpha_2 T_{21}$, QED gauge invariance strongly suppresses the amplitude for small photon energy. This leads to a relative enhancement of the $\alpha_1 T_{11}$ contribution away from the narrow $f_0(980)$ peak that is essential for obtaining a good fit, as seen by comparing Figs. 4c,d.

This same photon momentum effect impacts on the determination of the value of the coupling g_ϕ and of BR($\phi \to \gamma f_0$), making them both extremely sensitive to the exact position of the $f_0(980)$ pole, as we emphasise in the next section.

5 Widths and branching ratios

Most authors, instead of specifying the $\phi \to \gamma f_0$ coupling, quote the partial widths and finally the branching ratio BR($\phi \to \gamma f_0$). Then to calculate widths and branching ratios one has to rely on model-dependent assumptions about the resonance line shape. For instance, one could simply assume

$$\Gamma_\phi = \frac{1}{m_R} \rho_\phi(m_R^2) |g_\phi(s_R)|^2 \qquad (17)$$

using the value of g_ϕ as determined by the pole residue, where the pole position is parametrised by $s_R = m_R^2 - im_R\Gamma_t$. Nevertheless, to take into account the features of $F(s)$ in the neighbourhood of the f_0 resonance pole (in particular its finite width), we use a more refined formula which expresses the width Γ as an average of the product of the phase space ρ_ϕ times the square of the g_ϕ coupling integrated over the f_0 resonance density

$$\Gamma_\phi = \frac{\Gamma_t}{\pi} \int_{s_{\pi\pi}}^{m_\phi^2} ds \, \frac{\rho_\phi(s) |g_\phi(s_R)|^2}{|s - s_R|^2}, \qquad (18)$$

where $s_{\pi\pi}$ is the $\pi\pi$ threshold value of s, and for $s < m_\phi^2$ (cf. (7))

$$\rho_\phi(s) = \frac{\pi^2}{2m_\phi^3}(m_\phi^2 - s)\sqrt{s}. \qquad (19)$$

This would be the obvious procedure for integrating over the finite width of a resonance, if the resonance was isolated. But here the tail of the f_0 is not given by any Breit–Wigner shape, since it is intrinsically linked with the σ as required by unitarity for overlapping resonances. Consequently, data never show a pure f_0 line shape. So in this case the definition of widths and branchings involving the f_0 introduce a *strong* model dependence in the calculation. Once again we stress that it would be wiser to compare values of the $\phi \to \gamma f_0$ coupling calculated in different schemes as the residue of the resonance pole rather than relying on the branching ratio.
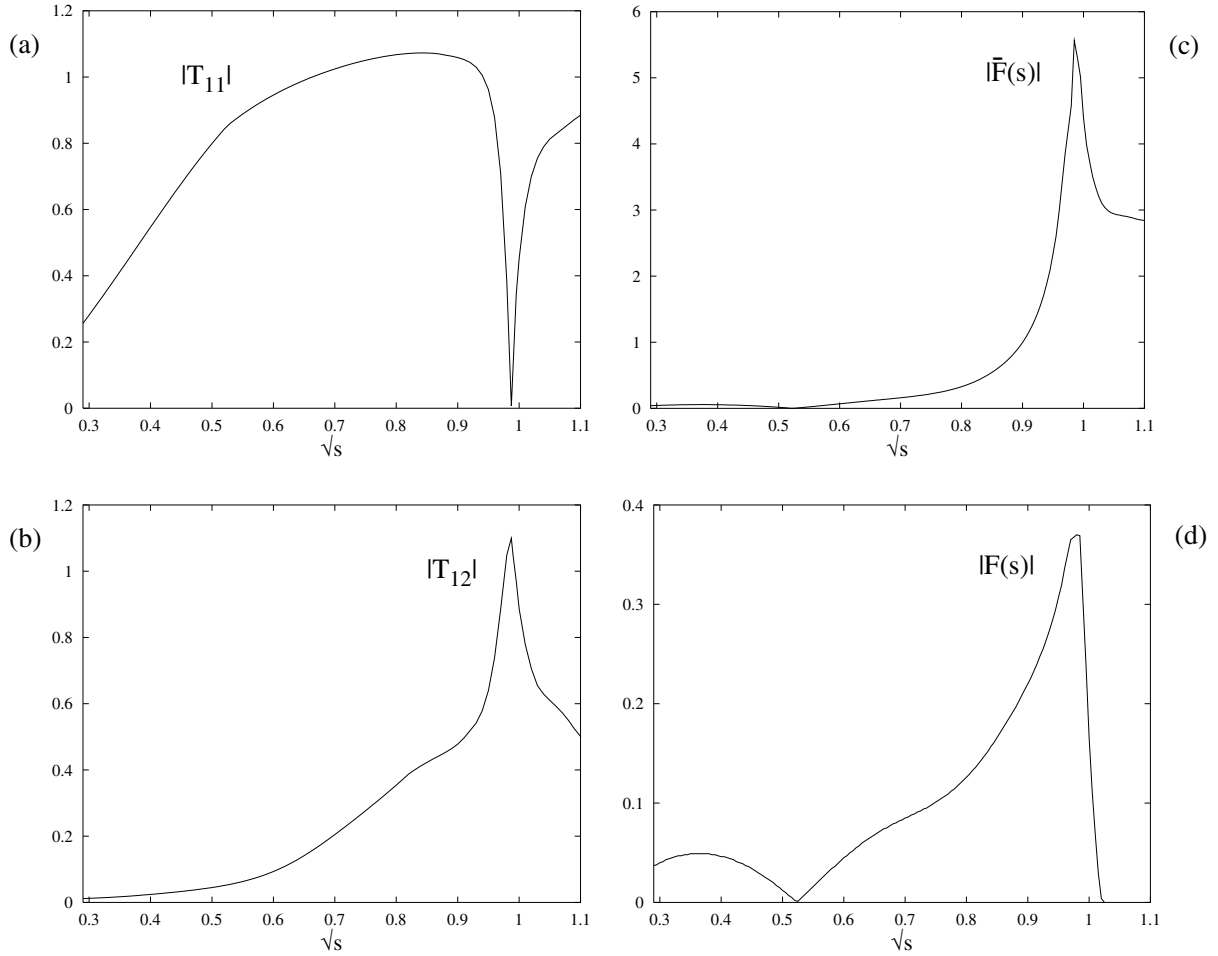
Fig. 4a–d. These diagrams illustrate the suppression of the $\phi \to \gamma\pi\pi$ decay amplitude, $F(s)$, as a function of di-pion mass $\sqrt{s}$ due to photon emission. Plots **a** and **b** show the ReVAMP hadronic amplitudes $|T_{11}|$ and $|T_{12}|$ from which $F(s)$ is constructed, according to (3). Plot **c** shows the amplitude $|\overline{F}(s)|$ one would obtain if the photon momentum factor $k \propto (1 - s/m_\phi^2)$ was divided out from the $\alpha_{1,2}$. Plot **d** shows the amplitude $|F(s)|$ itself, as determined by our fit using the parametrisation of (7) for the $\alpha_{1,2}$ coefficients. It is immediately clear that the photon momentum dramatically changes the di-pion mass distribution. Its effect is particularly striking in the region around 1 GeV, where the peak in $\overline{F}(s)$ is very narrow and spiky. Moreover, while $|\overline{F}(s)|$ slopes down gently beyond 1 GeV, $|F(s)|$ plummets to zero as $k \to 0$. This illustrates why the exact position of the $f_0(980)$ pole has such a strong effect on the coupling and branching ratio for $\phi \to \gamma f_0(980)$

Notice also that whether one uses the definition of decay width from (17) or from (18) is optional for the fits based on ReVAMP amplitudes, but the choice of (18) is inevitable when AS underlying amplitudes are used, since there the f_0 pole occurs at an energy larger than m_ϕ, where $\rho_\phi(s) = 0$.

A suitable normalization has to be chosen for the integral in (18): we use the Γ_t defined from the imaginary part of the pole position for the $f_0(980)$, which ensures consistency in calculating all the relevant partial widths in this process: Γ_ϕ, Γ_π and Γ_K. We do not renormalize our partial widths so that the sum of $\Gamma_\pi + \Gamma_K$ so defined equals Γ_t from the pole position as, for example, the authors of [13] do.

Table 4 shows the branching ratio corresponding to the pole-determined couplings, g_ϕ, of the two different fits. To understand why the values differ so much, even though the fits look very similar, we have to take a step back and understand the differences between the ReVAMP and the AS underlying amplitudes.

There the pole position relative to the $f_0(980)$ resonance is identified by continuing the T amplitudes into the complex plane, whereas the partial widths are obtained from formulae analogous to (18):

$$\Gamma_\pi = \frac{\Gamma_t}{\pi} \int_{s_{\pi\pi}} ds \, \frac{\rho_\pi(s) \, g_\pi^2(s_R)}{|s - s_R|^2} \, , \qquad (20)$$

$$\Gamma_K = \frac{\Gamma_t}{\pi} \int_{s_{K\overline{K}}} ds \, \frac{\rho_K(s) \, g_K^2(s_R)}{|s - s_R|^2} \, , \qquad (21)$$

where $s_{\pi\pi}$ and $s_{K\overline{K}}$ denote the $\pi\pi$ and $K\overline{K}$ threshold values of s, and

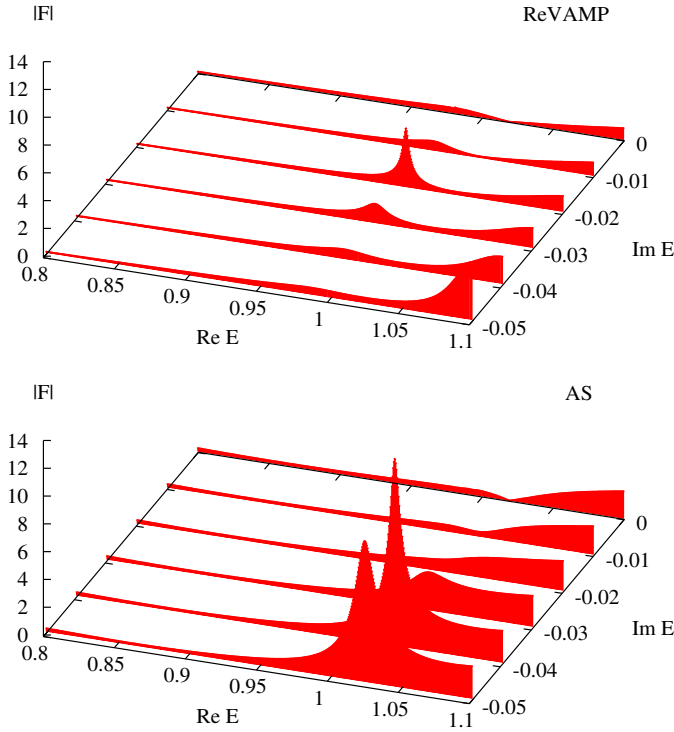$$\rho_\pi(s) = \sqrt{1 - 4m_\pi^2/s} \, , \qquad (22)$$

Fig. 5. Three-dimensional representation of the amplitude $|F|$ as a function of energy, E. This plot shows how the amplitude changes when continued to complex values of E past the $f_0(980)$ pole on the second Rieman sheet. Note that in the AS scheme (lower diagram) the $f_0(980)$ appears as a broad and pronounced peak, which shows up over more than one slice. On the same scale, the ReVAMP $f_0(980)$ corresponds to a much narrower and lighter resonance with a much more localized effect in the $|F(E)|$ profile (upper diagram)

$$\rho_K(s) = \frac{1}{2} \left[\sqrt{1 - 4m_{K^0}^2/s} + \sqrt{1 - 4m_{K^+}^2/s} \right]. \quad (23)$$

As we discussed in Sect. 1, the $f_0(980)$ is a much broader and heavier object in the AS amplitudes than in ReVAMPs. Now, the effect of such a broader resonance in the AS scheme is not that evident on the real axis, but becomes very relevant when moving into the complex s plane past the pole. This effect is transmitted to $F(s) = \alpha_1 T_{11} + \alpha_2 T_{12}$. On the real axis, where the fits to experimental data are performed, the $F(s)$ amplitudes obtained in the two different schemes look very similar, but the similarities fade away as soon as we leave the real axis to move into the complex plane, where the couplings are computed. This is demonstrated in Fig. 5 where the modulus of $F(s)$ is plotted against the real and imaginary part of $E = \sqrt{s}$ in a 3-dimensional plot. Slices of $|F(E)|$ at constant values of Im E show the profile of $|F|$ when moving further and further into the second Rieman sheet, as the pole corresponding to $f_0(980)$ takes shape and becomes the dominant feature in that energy range. By comparing the two plots one can readily see the differences between the two cases: for ReVAMP the pole is narrow and spiky and it occurs below the mass of the ϕ, very close to the $K\overline{K}$ threshold and not very far into the complex E plane.

On the contrary, the AS pole is a much broader structure, which occurs at energies higher than m_ϕ and twice as far from the real axis. These crucial differences explain why the couplings g_ϕ and branching ratios BR($\phi \to \gamma\pi\pi$) (shown in Table 4) calculated with two sets of underlying amplitudes differ so much.

We can now compare the values for the g_ϕ coupling and the $\phi \to \gamma f_0$ branching ratio we find from our analysis to the numbers obtained by various modellings of the ϕ decay into γf_0. First we consider the decay as if it only occurred through $K\overline{K}$ loops, i.e. $\phi \to \gamma K\overline{K} \to \gamma f_0$, as computed in the models of [1, 2, 20, ?, 22, 6].

By applying the earlier models of [1,2], in correspondence to the f_0 pole positions given by ReVAMP and AS, one would indeed find very small values of the $\phi \to \gamma f_0$ branching ratio, of order $< O(10^{-6})$, consistent with Table 1.

In a more recent $K^+ K^-$ loop calculation, Markushin presents a study of $\phi \to \gamma\pi\pi$ decay in a coupled-channel model containing the $\pi\pi$, $K\overline{K}$ and $q\overline{q}$ channels [21]. There he finds an $f_0(980)$ dynamically generated pole (i.e. a pole which disappears in the large N_c limit) corresponding to a molecular-like $K\overline{K}$ state. Nevertheless, the branching ratio he quotes is BR($\phi \to \gamma\pi^0\pi^0) = 3.5 \cdot 10^{-4}$, of the same order of magnitude as the older calculation would ascribe to a four-quark state!

Similarly, in [6] Oller presents the latest update of a calculation of the $\phi \to \gamma f_0$ branching ratio [22] based on a $K\overline{K}$ loop model for ϕ decays into two pseudoscalar mesons unitarising chiral perturbation theory. In this paper though [6], a $\phi\gamma K^0\overline{K}^0$ contact vertex is added to the $K\overline{K}$ loop diagrams and finite width effects of the intermediate resonance are taken into account. This leads him to find a branching ratio BR($\phi \to \gamma f_0$) even larger than Markushin's value. However, Oller notes, as we have, that the cubic dependence of the decay width on photon momentum can alter the branching ratio by a factor two if the resonance mass is varied by just 5 MeV!

Our analysis is more general than these specific meson loop calculations, since it does not restrict ϕ to decay through a particular channel, but it allows for any possible decay mechanism. Nevertheless, in the limit in which only the $T_{21}(K\overline{K} \to \pi\pi)$ underlying amplitude is used in (3) for constructing $F(s)$, we can expect our calculation to somehow reflect the modelling of [1, ?, 20–22, 6]. In this particular case, we find BR($\phi \to \gamma f_0) = 0.6 \cdot 10^{-4}$ for ReVAMP and BR($\phi \to \gamma f_0) = 1.9 \cdot 10^{-4}$ for AS, cf. Table 4. Although the fits do not appear too bad when plotted against the data, their χ^2/d.o.f. are in the range of 4–5, so they are not included in Table 5.

Finally, we compare our results to those reported in the data analyses by the KLOE [7] collaboration at DAΦNE and by the CMD-2 [3] and SND [4,5] collaborations at VEPP-2M. These are summarised in Table 5. KLOE, CMD-2 and SND approach to the problem is based on fitting dBR($\phi \to \gamma\pi^0\pi^0$)/d$M_{\pi\pi}$ data with some appropriate Breit–Wigner forms for the f_0 and the σ resonances. The branching ratio is then computed as the area underneath the curve determined by the fit. All their evaluations give

Table 5. Values of the branching ratio BR($\phi \to \gamma f_0$) as calculated by the KLOE [7], CMD-2 [3] and SND [4,5] collaborations compared with those obtained in our determination using the ReVAMP [12] and AS [13] underlying hadronic amplitudes

	BR($\phi \to \gamma f_0$) $\cdot 10^4$
KLOE	(4.47 ± 0.21)
CMD-2	$(2.90 \pm 0.21 \pm 1.54)$
SND	$(3.42 \pm 0.30 \pm 0.36)$
SND – reanalysis	$(3.5 \pm 0.3^{+1.3}_{-0.5})$
ReVAMP-0 (fit to KLOE + SND)	0.31
ReVAMP-II (fit to KLOE + SND)	0.34
AS-II (fit to KLOE + SND)	1.92

similar results because they all closely follow the same prescription, [20]: again, ϕ decays into γf_0 are modelled as if they proceed through K^+K^- loops only. The mass spectrum is represented as a sum of three terms, one representing the decay of ϕ to two pions through a scalar resonance, one taking into account the $\rho\pi$ background and one corresponding to the interference between them. The mass of the f_0 together with the $g_{\phi K^+K^-}$ and $g_{f_0\pi^+\pi^-}$ couplings are free parameters to be determined by the fit, whereas the mass and width of the σ are fixed. Once again we stress that modelling the $\pi\pi$ S-wave spectrum, characterized by wide overlapping and interfering resonances, with a Breit–Wigner form is totally inconsistent with unitarity. In fact, the values of the $g_{\phi K^+K^-}$ and $g_{f_0\pi^+\pi^-}$ couplings they find are very large, leading to a disproportionately wide $f_0(980)$: $\Gamma_{\pi\pi} \sim 150$–250 MeV!

6 Conclusions

We have shown that *there is* a model-independent way to determine the $\phi \to \gamma f_0$ coupling g_ϕ, which we believe is the only rigorously correct way to treat S-wave interactions, where the underlying resonances are far from Breit–Wigner-like. It is based on unitarity, which gives strong constraints below 1 GeV where the $\pi\pi$ channel is effectively the only open channel and it ensures universality of di-pion final state interactions through Watson's theorem. The results for g_ϕ are given in Table 4 and for the branching ratio in Table 5.

ϕ-radiative decay to the $f_0(980)$ in principle provides a way of determining the internal composition of this enigmatic scalar. Models give quite different predictions for a $qq\overline{q}\overline{q}$ or $s\overline{s}$ state, with a range of predictions for a $K\overline{K}$ molecule. Long before experimental data on ϕ-radiative decays became available, Achasov [1] stressed that they would reflect QED gauge invariance with the decay distribution being proportional to the cube of the photon momentum. He further emphasised that models must incorporate this behaviour too [19]. We have seen that these momentum factors make ϕ-radiative decay a very difficult tool for unravelling the structure of the $f_0(980)$. The strong suppression as $\pi\pi$ mass approaches m_ϕ makes the

$\phi \to \gamma f_0$ coupling, g_ϕ, very strongly dependent on the $f_0(980)$ mass and width. At present, analyses of the underlying hadronic processes allow a sizeable variation to occur in these parameters (see Table 4). This is particularly so because of our poor knowledge of $K\overline{K} \to \pi\pi$ scattering, as emphasised long ago, for instance in [12].

Nevertheless, the underlying dynamics of the decay is clear. $\pi\pi$ and $K\overline{K}$ are the only hadronic intermediate states relevant to spin zero interactions below the ϕ mass. Consequently, the decay $\phi \to \gamma\pi\pi$ can only proceed either by the coupling α_1 of $\phi \to \gamma\pi\pi$ followed by $\pi\pi$ interactions or the coupling α_2 for $\phi \to \gamma K\overline{K}$ followed by the $K\overline{K}$ system producing a $\pi\pi$ final state. Given the fact that the ϕ is overwhelmingly an $s\overline{s}$ system, we expect the coupling α_2 that picks out the $K\overline{K} \to \pi\pi$ scattering component to dominate. That it does is perfectly illustrated in Fig. 4. Recall Fig. 4c shows $\overline{F}(s)$, the $\phi \to \gamma\pi\pi$ amplitude with the photon momentum divided out. This is seen to look very like T_{12}, the $K\overline{K} \to \pi\pi$ amplitude, particularly in the 0.95 to 1 GeV region. The $\pi\pi \to \pi\pi$ component, T_{11}, is small but not negligible below 900 MeV. Multiplying the amplitude $\overline{F}(s)$ by the photon momentum factor $k \propto (1 - s/m_\phi^2)$ (required by QED gauge invariance) to get the full amplitude suppresses the contribution of the $K\overline{K} \to \pi\pi$ component with its spiky peak close to 1 GeV and enhances lower masses where $\pi\pi \to \pi\pi$ interactions dominate. For instance, the photon momentum enhances the region at 900 MeV by nearly a factor 3 relative to the peak at 980 MeV, and so in the decay distribution, where the photon momentum appears cubed, by a relative factor of 24. Looking at the underlying hadronic amplitudes displayed in Figs. 4a,b shows why the peak in the ϕ-radiative decay distribution in the $\pi\pi$ channel is so much wider than the 50 MeV of the $f_0(980)$. Thus models that neglect the $\phi \to \gamma(\pi\pi \to \pi\pi)$ contribution fail to reproduce the decay distribution accurately.

The KLOE experimental integrated branching ratio is

$$\text{BR}(\phi \to \gamma\pi^0\pi^0) = (1.09 \pm 0.03 \pm 0.05) \cdot 10^{-4}.$$

An $f_0(980)$ with conventional parameters of mass 989 MeV and width 44 MeV, as incorporated in the ReVAMP amplitudes, gives BR($\phi \to \gamma f_0 \to \gamma\pi^0\pi^0$) = $0.11 \cdot 10^{-4}$ which is only 10% of this total distribution. The remaining 90% is from the decay through the broad $f_0(400$–$1200)$ (or σ). This is large wholly because of the larger phase space and the photon momentum factors. The coupling to this intrinsically non-strange system is comparable to that expected from the branching ratio of $\phi \to \rho\pi$. In this case, the coupling of the $\phi \to \gamma f_0$ is much smaller than predicted in models with $qq\overline{q}\overline{q}$ structure for the $f_0(980)$, but rather in agreement with an $s\overline{s}$ structure or within the newly extended range for a $K\overline{K}$ molecule [6]. In contrast, the underlying AS amplitudes, which embed a wider and heavier f_0, give BR($\phi \to \gamma\pi^0\pi^0$) = $0.64 \cdot 10^{-4}$ which is 40% of the experimental branching ratio and closer to that for a $qq\overline{q}\overline{q}$ composition, but the χ^2 for these fits are significantly worse (Table 3).

To determine the corresponding coupling $\phi \to \gamma a_0$ would require a similar coupled-channel analysis of the

$\gamma\eta\pi$ decay mode, in which one should include information on the hadronic channels $\pi^0\eta \to \pi^0\eta, K\overline{K}$, but precise information is lacking on the latter channel. Nevertheless, the $a_0(980)$ has none of the complications of the $f_0(980)$, in that the resonance does not overlap with any other broad structure. Consequently, one can anticipate that the branching ratio determined by the experimental groups [3–5,7] are correct within a small factor. We can, therefore, conclude from our analysis that the $\phi \to \gamma f_0(980)$ coupling will be of the same order of magnitude as that for $\phi \to \gamma a_0(980)$. Although in a simple model with only K^+K^- loops one would naively expect the ratio of these branching ratios to be one, we know that this is extremely sensitive to the exact position of the resonance poles corresponding to the a_0 and f_0. Thus, it is the ratio of the couplings that reflects the dynamics of these decays and should be used as a guide to the composition of these mesons. The ratio of branching ratios would be a clear guide if these scalar states were to be seen in $\phi(1680)$ decay, when they would not be close to the end of phase space.

Present ϕ decay data do favour the conventional narrow $f_0(980)$ as in the ReVAMP scheme [12]. Nevertheless, we do need to fix $T_{11}(\pi\pi \to \pi\pi)$ and $T_{12}(\pi\pi \to K\overline{K})$ in the 1 GeV region very accurately before we can reach definite conclusions about the $\phi \to \gamma f_0$ coupling and its consequences for the structure of the $f_0(980)$. Further direct information on T_{11} and T_{12} is unlikely, so to achieve the required precision we need either a careful and exhaustive analysis of the D_s decay data, which are presently being accumulated, or yet higher statistics results on ϕ-radiative decay with fine resolution close to 1 GeV. In either case, these data can only fix the $f_0(980)$ parameters if they are analysed in a way consistent with all other sources of information in harmony with unitarity. The necessary data are at last becoming available. How to analyse these has been described here. The outcome should be clear within 12 months.

References

1. N.N. Achasov, V.N. Ivanchenko, Nucl. Phys. B **315**, 465 (1989)
2. S. Nussinov, T.N. Truong, Phys. Rev. Lett **63**, 1349 (1989); J. Lucio, J. Pestieau, Phys. Rev. D **42**, 3253 (1990); F.E. Close, N. Isgur, S. Kumano, Nucl. Phys. B **389**, 513 (1993); N. Brown, F.E. Close, The DAΦNE Physics Handbook, edited by L. Maiani, G. Pancheri, N. Paver, INFN, Frascati (1995) pp. 447–464
3. R.R. Akhmetshin et al., Phys. Lett. B **462**, 380 (1999)
4. M.N. Achasov et al., Phys. Lett. B **440**, 442 (1998)
5. M.N. Achasov et al., Phys. Lett. B **485**, 349 (2000)
6. J.A. Oller, Nucl. Phys. A **714**, 161 (2003)
7. A. Aloisio et al., Phys. Lett. B **537**, 21 (2002)
8. A. Aloisio et al., Phys. Lett. B **536**, 209 (2002)
9. J.A. Oller, E. Oset, Nucl. Phys. A **620**, 438 (1997); Erratum A **652**, 407 (1999)
10. S. Ishida et al., Prog. Theor. Phys. **95**, 745 (1996); **98**, 1005 (1997); S. Ishida, Proceedings of the 7th International Conference on Hadron Spectroscopy (Hadron 97), Upton, NY, August 1997, pp. 705; T. Ishida et al., ibid., p. 385; Proceedings of the Workshop on Hadron Spectroscopy, Rome, Italy, March 1999, pp. 85; M. Ishida et al., ibid., p. 115; hep-ph/0212383; Nuclear Medium, Kyoto, Japan, October 2002, hep-ph/0212383
11. K.L. Au, D. Morgan, M.R. Pennington, Phys. Rev. D **35**, 1633 (1987)
12. D. Morgan, M.R. Pennington, Phys. Rev. D **48**, 1185 (1993)
13. V.V. Anisovich, A.V. Sarantsev, hep-ph/0204328
14. V.V. Anisovich, Proceedings of the 7th International Conference on Hadron Spectroscopy (Hadron 97), Upton, NY, August 1997, pp. 421–432
15. W. Ochs, Ph.D. Thesis, Munich University (1973), unpublished; B. Hyams et al., Nucl. Phys. B **74**, 134 (1973)
16. J. Gunter et al., Phys. Rev. D **64**, 072003 (2001)
17. S. Pislak et al., Phys. Rev. Lett. **87**, 221801 (2001)
18. W. Hoogland et al., Nucl. Phys. B **126**, 109 (1977)
19. N.N. Achasov, AIP Conf. Proc. **619**, 112 (2002); also in the Conference proceedings of the 9th International Conference on Hadron Spectroscopy (Hadron 2001), Protvino, Russia, August 2001, pp. 112–121
20. N.N. Achasov, V.V. Gubin, Phys. Rev. D **63**, 094007 (2001)
21. V.E. Markushin, Eur. Phys. J. A **8**, 389 (2000)
22. J.A. Oller, Phys. Lett. B **426**, 7 (1998); E. Marco et al., Phys. Lett. B **470**, 20 (1999)